Synthesis and Crystal Structure of a Mn(II) Metal-Organic Framework Based on a Polydentate Schiff Base Ligand

Jun Li Wang, Hai Yan Li, Chen Hong Liu, and Yan Bai

Reprint requests to Dr. Yan Bai. Fax: +86-378-3881589. E-mail: baiyan@henu.edu.cn

Z. Naturforsch. **2013**, *68b*, 351 – 356 / DOI: 10.5560/ZNB.2013-3037
Received February 7, 2013

A Mn(II) metal-organic framework $\{[MnL_2(NCS)_2]\cdot(H_2O)_4\}_n$ (**1**) with L = bis(pyridin-3-yl-methylene)biphenyl-2,2′-dicarbohydrazide has been synthesized and characterized by IR spectroscopy, elemental analysis, UV spectroscopy, thermogravimetric (TG) analysis, powder X-ray diffraction, and single-crystal X-ray structure determination. The Mn(II) atom has a distorted octahedral coordination environment with an N_6 donor set from four ligands and two NCS^- anions. The structure of **1** exhibits a layer framework containing tetranuclear metallacyclic ring units $[Mn^{II}{}_4L_4]$ in the chair conformation. In addition, there are multiform O–H···O, C–H···O, N–H···O, and C-H···N hydrogen bonds and C–H···π interactions in a three-dimensional supramolecular network.

Key words: Manganese(II), Metal-Organic Framework, Schiff Base, Crystal Structure

Introduction

Recently, much interest in self-assembly of metal-organic frameworks (MOFs) with intriguing topologies has grown rapidly owing to their potential applications in catalysis, molecular adsorption, magnetism, optical devices and molecular sensors [1 – 3]. In particular, the incorporation of Mn(II) into metal-organic frameworks has received increasing attention in the fields of supramolecular chemistry and crystal engineering for the remarkable performances of the products in magnetical systems, catalysis and biochemistry [4, 5]. Generally, the syntheses of MOFs are based on a self-assembly of organic ligands and metal ions or clusters, counterions, and solvent systems [6, 7]. Among them, the design of organic ligands is the most important element for assembling MOFs with novel topologies. Neutral, rigid *N*-donor ligands have been widely used to construct MOFs along with various anionic species to balance the electrostatic equilibrium of the networks [8 – 11]. Biphenyl-based Schiff base ligands are one type of ligands to assemble different structural frameworks [12 – 15], such as helical structures imposed by constrained rotation around the C-C bond of these otherwise flexible ligands [16, 17]. Consequently, the ligands with a twist conformation could be used as potential helical building blocks to synthesize frameworks with corresponding architectures [18 – 21]. In comparison with previously reported ligands like *N*′,*N*′-bis[1-(pyridin-4-yl)methylidene]benzyl dihydrazone (L^1) and *N*′,*N*′-bis[1-(pyridin-3-yl)methylidene]benzyl dihydrazone (L^2) [14], the ligand bis(pyridin-3-yl-methylene)biphenyl-2,2′-dicarbohydrazide (L) selected here not only possesses a longer spacer to separate the two pyridyl binding sites, but also may link metal ions *via* additional donor sites, *viz.* two pyridyl N donors, two imine N donors, two amine N donors and two carbonyl O donors, to generate multidimensional frameworks [22]. In addition, the linear triatomic pseudohalide SCN^- is a frequently used anionic auxiliary ligand, which can coordinate through either the S or N atom to a metal center [23 – 28]. In the present paper, through the assembly of the biphenyl-based Schiff base ligand L, the SCN^- anion and the Mn(II) cation, a two-dimensional MOF $\{[MnL_2(NCS)_2]\cdot(H_2O)_4\}_n$ (**1**) was synthesized and characterized especially by single-crystal X-ray diffraction analysis.

Experimental Section

General

Materials: All chemicals were of reagent grade quality obtained from commercial sources and used without further

purification. Ligand L was synthesized and characterized by a previously reported procedure [22].

Instrumentation: Elemental analyses (C, H and N) were carried out on a Perkin-Elmer 240C analytical instrument. IR spectra were recorded from KBr pellets with a Nicolet 170 SXFT-IR spectrophotometer in the 4000 – 400 cm^{-1} region. The UV/Vis spectrum was measured in H_2O solution with a Hitachi U-4100 spectrophotometer. Powder X-ray diffraction patterns were recorded on a D/max-γ A rotating anode X-ray diffractometer with a sealed Cu tube ($\lambda = 1.54178$ Å). The thermogravimetric analysis (TGA) of coordination polymer **1** was carried out under nitrogen on a Perkin-Elmer-7 thermal analyzer at a heating rate of 10 °C min^{-1} from 25 to 700 °C.

Synthesis

10 mL of an acetonitrile solution of $MnCl_2 \cdot 4H_2O$ (59 mg, 0.3 mmol) and 2 mL of an aqueous solution of KSCN (90 mg, 0.9 mmol) were mixed; the solution was filtered and added to 10 mL of a methanol solution of L (45 mg, 0.1 mmol). The excess of manganese salts used here was used to improve the yield based on the ligand. The resulting mixture was stirred for 0.5 h and left to slowly evaporate at room temperature to obtain yellow block-shaped crystals suitable for single-crystal X-ray diffraction. The bulk samples were further purified by recrystallization from acetonitrile-methanol. The total yield was 60 % (34 mg) based on ligand L. – Anal. for $C_{54}H_{48}MnN_{14}O_8S_2$: calcd. C 56.89, H 4.24, N 17.20; found C 57.10, H 4.17, N 17.25. – IR (cm^{-1}, KBr pellet): $v = 3446$(m), 3190(w), 2996(w), 2851(w), 2053(s), 1652(s), 1613(m), 1600(m), 1570(m), 1474(m), 1419(m), 1361(m), 1304(s), 1274(w), 1193(w), 1156(s),1112(m), 1098(w), 1064(w), 1045(w), 938(w), 925(w), 853(m), 763(m), 711(m), 640(w), 558(w).

X-Ray crystallographic study

A suitable single crystal of size $0.34 \times 0.23 \times 0.10$ mm^3 was chosen for the crystallographic study and then mounted on a Bruker Smart APEX II CCD diffractometer with ω- and ϕ-scan mode in the range of $1.91 \leq \theta \leq 25.00°$. All diffraction measurements were performed at room temperature using graphite-monochromatized MoK_α radiation ($\lambda = 0.71073$ Å). The structure was solved by Direct Methods and refined on F^2 by using full-matrix least-squares methods with SHELXS/L-97 [29, 30]. All non-hydrogen atoms were refined anisotropically by full-matrix least-squares techniques. All hydrogen atoms were geometrically fixed to allow riding on the parent atoms to which they are attached, except those disordered hydrogen atoms which were added to the molecular formula according to the electroneutrality principle. To assist the refinement, the water oxygen atom O2W was taken as rotationally disordered over three orientations in the refined ratio 0.5 : 0.25 : 0.25. Space group, lattice parameters and other relevant information are listed in Table 1, and selected bond lengths and angles are given in Table 2.

Table 1. Summary of crystal data and refinement results for the title compound.

Chemical formula	$C_{54}H_{48}MnN_{14}O_8S_2$
Formula weight	1140.12
Temperature, K	296(2)
Crystal system	monoclinic
Space group	$P2_1/c$
Unit cell dimensions	
a, Å	11.0127(13)
b, Å	12.4725(15)
c, Å	20.454(2)
β, deg	91.237(2)°
Volume, Å^3	2808.8(6)
Z	2
D_{calcd}, g cm^{-3}	1.35
$F(000)$, e	1182
μ, mm^{-1}	0.4
θ range data collection, deg	1.91–25.00
Index ranges *hkl*	$-13 \leq h \leq 12$, $-14 \leq k \leq 14$, $-13 \leq l \leq 24$
Refl. collected / unique / R_{int}	14 103 / 4948 / 0.0527
Data/parameters	4948 / 361
Goodness of fit on F^2	1.008
$R1(F)$ / $wR2(F^2)$ [$I > 2\sigma(I)$]	0.0510 / 0.1219
$R1(F)$ / $wR2(F^2)$ (all data)	0.1140 / 0.1385
Largest diff. peak / hole, e Å^{-3}	0.41 / −0.46

Table 2. Selected bond lengths (Å) and angles (deg) of the title compound.[a]

Bond lengths			
Mn(1)–N(1)	2.169(3)	Mn(1)–N(7B)	2.303(3)
Mn(1)–N(2)	2.319(3)		
Bond angles			
N(1)–Mn(1)–N(7B)	91.14(11)	N(1)–Mn(1)–N(7C)	88.86(11)
N(1)–Mn(1)–N(2)	87.82(12)	N(1)–Mn(1)–N(2A)	92.18(12)
N(7B)–Mn(1)–N(2)	92.40(10)	N(7C)–Mn(1)–N(2)	87.60(10)

[a] Symmetry codes: A: $-x+2, -y+1, -z$; B: $-x+1, y-1/2, -z-1/2$; C: $x+1, -y+3/2, z+1/2$.

CCDC 906891 contains the supplementary crystallographic data. These data can be obtained free of charge from The Cambridge Crystallographic Data Centre *via* www.ccdc.cam.ac.uk/data_request/cif.

Results and Discussion

IR and UV/Vis spectra

In the IR spectrum of polymer **1**, the absorption bands at 1652 and 1613 cm^{-1} are assigned to

the C=O and C=N group, respectively, which are shifted slightly to higher wavenumbers compared with L (1651 and 1593 cm^{-1}). The sharp and strong absorption band at 2053 cm^{-1} should be attributed to ν(SCN), indicating nitrogen coordination of the NCS^- group [31 – 34]. These assignments were finally confirmed by X-ray crystallography (see below). The UV spectrum of **1** in aqueous solution displays two absorption peaks at 196 and 284 nm, respectively, which can be assigned to the π-π^* and n-π^* transitions of ligand.

Crystal and molecular structure

In the solid state the title compound forms a 2D coordination polymer. The asymmetric unit consists of one half Mn(II) atom which lies on an inversion center, one ligand L, one NCS^- anion and two H_2O molecules. As shown in Fig. 1, the coordination sphere around the manganese atom is distorted octahedral made up of four $N_{pyridyl}$ donor atoms from four ligands and two N_{NCS} donor atoms. The axial Mn(II)–N_{NCS} bond length of 2.169(3) Å is shorter than the equatorial Mn(II)–$N_{pyridyl}$ distances of 2.303(3) and 2.319(3) Å. Through two $N_{pyridyl}$ donors the bidentate ligand bridges two Mn(II) centers with a separation of 16.121(2) Å for Mn(1)···Mn(1D) (symmetry code D: $1-x$, $1/2+y$, $-1/2-z$). Four ligands bridge four Mn(II) centers to obtain a tetranuclear metallacycle $[Mn^{II}{}_4L_4]$ in the chair conformation with one large Mn···Mn separation of 29.733(3) Å and one shorter Mn···Mn separation of 12.472(2) Å (Fig. 2). Compared to the similar tetranuclear metallacyclic structure in $\{[ZnL^1{}_2(NCS)_2]CH_3CN\}_n$ ($L^1 = N',N'$-bis[1-(pyridin-4-yl)methylidene]benzyl dihydrazone), the separations of metal centers in four zeniths of the metallacycle $[Mn^{II}{}_4L_4]$ are longer owing to the longer spacer in L [20]. These macrometallacyclic units are further extended to form a layer network. In the solid state, H_2O molecules are tightly fitted into the tetranuclear metallacyclic rings through multiform O–H···O, C–H···O and N–H···O hydrogen bonds (Table 3). These H_2O molecules also link adjacent sheets by O(1W)–H(1WA)···O(1) hydrogen bonds forming a 3D supramolecular structure (Fig. 3).

It is worth pointing out that polymer **1** contains infinite 2_1 helical chains through the bridging of Mn(II) centers by the helical ligands. The helical pitch, given by one full rotation around the 2_1 helical axis, is 12.472(2) Å (the unit cell length along the crystallographic b axis). The axis of the helix runs at (0, y, 1/4). Complex **1** crystallizes in the centrosymmetric space group $P2_1/c$, and the metal ion occupies the crystallographic inversion center. Consequently, one P helicate and one M helicate are alternating in the layers (Fig. 4). The dihedral angle between two benzene rings of the twisted ligand is 74.4(2)°. The torsion angles about C(7)=N(3)–N(4)=C(8) and C(21)=N(5)–N(6)=C(22) bonds are 172.6(6) and 171.7(6)°, respectively. Two types of C(2)–H(2A)···N(3) and N(4)–H(4B)···O(2) intramolecular hydrogen bonds are found in the ligand, especially N(4)–H(4B)···O(2) from two arms of one ligand stabilizing the helical structure.

In addition, there is a C–H···N hydrogen bond between C(27) of the pyridyl ring and N(1) of the NCS^-

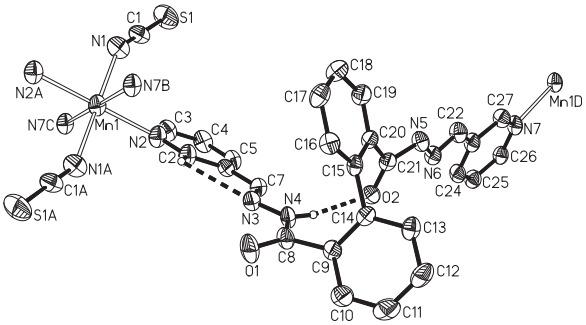

Fig. 1. ORTEP diagram of the coordination environment of the Mn(II) atoms in the coordination polymer **1** showing intramolecular hydrogen bonding as dashed lines. The displacement ellipsoids are at the 30% probability level. Symmetry codes: A: $-x+2$, $-y+1$, $-z$; B: $-x+1$, $y-1/2$, $-z-1/2$; C: $x+1$, $-y+3/2$, $z+1/2$; D: $-x+1$, $y+1/2$, $-z-1/2$.

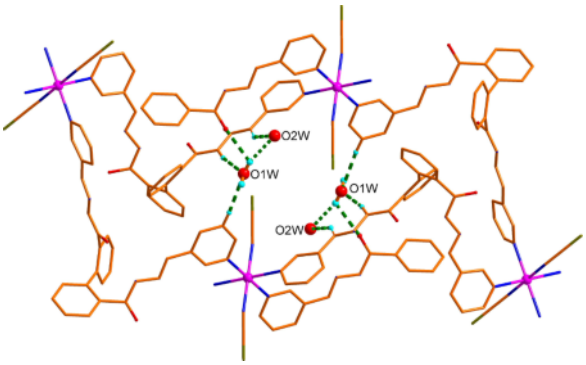

Fig. 2 (color online). Illustration of one tetranuclear metallacyclic unit $[Mn^{II}{}_4L_4]$ with H_2O molecules fitted into the large macrocycles through multiform hydrogen bonds.

Table 3. Hydrogen bond interactions (Å and deg) of the title compound.

D–H···A	*d*(D–H)	*d*(H···A)	*d*(D···A)	∠(DHA)	Symm. codes of atom A
O(1W)–H(1WA)···O(1)	0.85	2.56	3.392(5)	165	
O(1W)–H(1WB)···O(2W)	0.85	2.11	2.911(7)	157	$-x, 1/2+y, -1/2-z$
O(1W)–H(1WB)···O(1)	0.85	2.43	2.957(5)	121	$1-x, -y, -z$
N(4)–H(4B)···O(2)	0.86	2.01	2.845(3)	164	
N(5)–H(5B)···O(1W)	0.86	2.22	3.065(5)	168	$x, 1/2-y, -1/2+z$
C(2)–H(2A)···N(3)	0.93	2.55	2.863(4)	100	
C(4)–H(4A)···O(1W)	0.93	2.54	3.464(5)	173	$1-x, 1-y, -z$
C(22)–H(22A) ···O(2W)	0.93	2.57	3.391(7)	147	$-x, -y, -1-z$
C(27)–H(27A)··· N(1)	0.93	2.61	3.199(5)	122	$1-x, 1/2+y, -1/2-z$

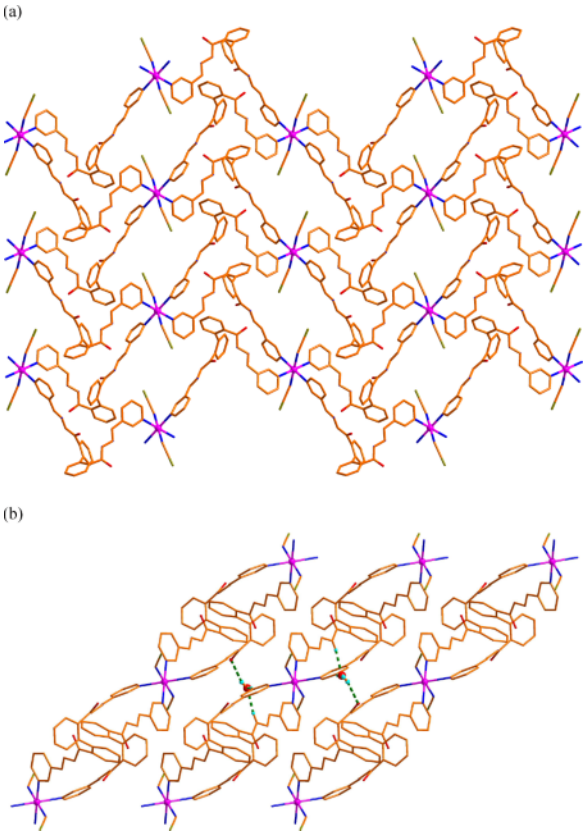

Fig. 3 (color online). (a) View of the sheets in the coordination polymer **1** containing tetranuclear metallacyclic units (H_2O molecules are omitted for clarity); (b) packing diagram of the 3D supermolecular frameworks with hydrogen bonds shown as dashed lines.

group. The C···N separation is 3.199(5) Å, and the C–H···N angle is 122° for C(27)–H(27A)···N(1). The C–H···π interaction between the carbon atom C(5) and the adjacent benzene ring [C(15D)–C(20D)] (D: $1-x$, $1/2+y$, $-1/2-z$) is characterized by the H···*M* separation and C–H···*M* angle of 2.96 Å and 127°, respectively (*M*, midpoint of the benzene ring). Although

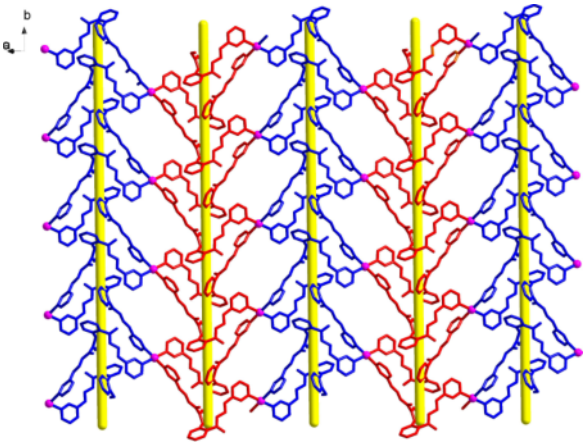

Fig. 4 (color online). View of the 2_1 helical chains in the coordination polymer **1** with blue chains representing right-handed helices and red chains representing left-handed helices (H_2O molecules omitted for clarity).

these hydrogen bonds and C–H···π interactions are exceedingly weak compared to the metal-nitrogen coordination bonds and the other more polar hydrogen bonds, it is suggested that these interactions are important in the packing of the molecules.

The powder X-ray diffraction (PXRD) measurement of polymer **1** was performed to check the phase purity of the samples. Most peak positions of simulated and experimental patterns correspond well with each other (Fig. 5), indicating that the bulk products of **1** are a pure phase. The dissimilarities in intensity may be due to the preferred orientation of the crystalline powder samples during collection of the experimental XRPD.

Thermogravimetric analysis

Thermogravimetric experiments were conducted to examine the thermal stability of the metal-organic compound. The curve of **1** suggests that the weight loss in the range from 36 to 115 °C is 6.22 %, corre-

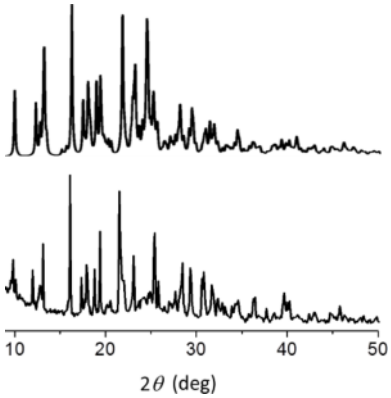

Fig. 5. The powder X-ray diffraction pattern calculated from the single-crystal data (top) and that obtained from the experiment (bottom) for **1**.

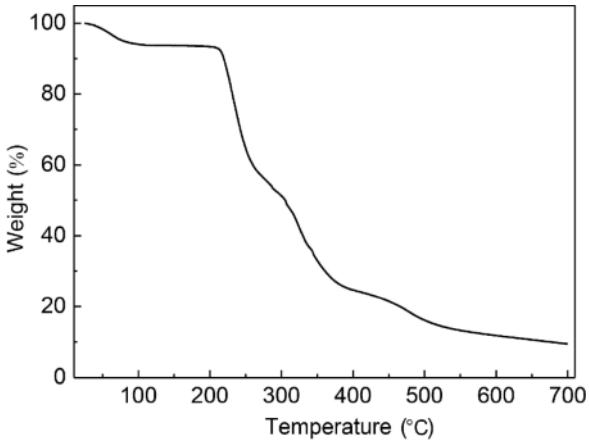

Fig. 6. Thermogravimetric analysis (TGA) for **1**.

sponding to the loss of four H_2O molecules (calcd. 6.32 %) (Fig. 6), which is in agreement with the formula $\{[MnL_2(NCS)_2]\cdot(H_2O)_x\}_n$ with $x = 4$ proposed above. Two ligands and two NCS^- anions are lost in a continuous fashion above 212 °C, and the decomposition of the framework backbone is still progressing even at the upper limit of measurement range.

Conclusions

In summary, we have presented a 2D coordination polymer $\{[MnL_2(NCS)_2]\cdot(H_2O)_4\}_n$ (**1**) based on the Schiff base ligand bis(pyridin-3-ylmethylene)biphenyl-2,2′-dicarbohydrazide (L). The crystal and molecular structure of **1** has been determined on single crystals. The complex was also characterized by IR spectroscopy, UV spectroscopy, PXRD and thermogravimetric (TG) analysis. The polymer shows a layer containing two types of 2_1 helical chains (*P* and *M* helices) formed by the bridging interactions of the twisted ligands with the Mn(II) centers.

Acknowledgement

This work was supported by the Natural Science Foundation of Henan Province of China, the Foundation of the Education Department of Henan Province of China and the Foundation co-established by the Province and the Ministry of Henan University.

[1] H. H. Wu, Q. H. Gong, D. H. Qison, J. Li, *Chem. Rev.* **2012**, *112*, 836 – 868.
[2] J. P. Zhang, Y. B. Zhang, J. B. Lin, X. M. Chen, *Chem. Rev.* **2012**, *112*, 1001 – 1033.
[3] S. M. Cohen, *Chem. Rev.* **2012**, *112*, 970 – 1000.
[4] P. Kar, R. Biswas, Y. Ida, T. Ishida, A. Ghosh, *Cryst. Growth Des.* **2011**, *11*, 5305 – 5315.
[5] D. B. Dang, B. An, Y. Bai, G. S. Zheng, J. Y. Niu, *Chem. Commun.* **2013**, *49*, 2243 – 2245.
[6] S. P. Jang, J. L. Poong, S. H. Kim, T. G. Lee, J. Y. Noh, C. Kim, Y. Kim, S. J. Kim, *Polyhedron* **2012**, *33*, 194 – 202.
[7] S. L. Cai, M. Pan, S. R. Zheng, J. B. Tan, J. Fan, W. G. Zhang, *CrystEngComm* **2012**, *14*, 2308 – 2315.
[8] S. Noro, R. Kitaura, M. Kondo, S. Kitagawa, T. Ishii, H. Matsuzaka, M. Yamashita, *J. Am. Chem. Soc.* **2002**, *124*, 2568 – 2583.
[9] C. Biswas, P. Mukherjee, M. G. B. Drew, C. J. Gómez-García, J. M. Clemente-Juan, A. Ghosh, *Inorg. Chem.* **2007**, *46*, 10771 – 10780.
[10] S. Hazra, B. Sarkar, S. Naiya, M. G. B. Drew, A. Frontera, D. Escudero, A. Ghosh, *Cryst. Growth Des.* **2010**, *10*, 1677 – 1687.
[11] M. S. Ray, A. Ghosh, A. Das, M. G. B. Drew, J. Ribas-Ariño, J. Novoa, J. Ribas, *Chem. Commun.* **2004**, 1102 – 1103.
[12] G. Q. Yang, M. Liu, X. P. Li, J. Li, J. S. Ma, *J. Coord. Chem.* **2009**, *62*, 3478 – 3487.
[13] B. Dede, F. Karipcin, M. Cengiz, *J. Chem. Sci.* **2009**, *121*, 163 – 171.
[14] Y. Bai, J. L. Wang, D. B. Dang, Y. N. Zheng, *Spectrochim. Acta, Part A, Mol. Biomol. Spectrosc.* **2012**, *97*, 105 – 110.

[15] D. B. Dang, J. D. Sun, Y. Bai, H. Gao, W. L. Shang, *J. Chem. Crystallogr.* **2009**, *39*, 683 – 687.
[16] Q. Z. Sun, M. L. Wei, Y. Bai, C. He, Q. J. Meng, C. Y. Duan, *Dalton Trans.* **2007**, 4089 – 4094.
[17] Q. Z. Sun, Y. Bai, G. J. He, C. Y. Duan, Z. H. Lin, Q. J. Meng, *Chem. Commun.* **2006**, 2777 – 2779.
[18] L. X. Xie, D. Y. Wu, C. Y. Duan, B. G. Zhang, Q. J. Meng, *Chin. J. Inorg. Chem.* **2007**, *23*, 191 – 199.
[19] D. B. Dang, G. S. Zheng, Y. Bai, F. Yang, H. Gao, P. T. Ma, J. Y. Niu, *Inorg. Chem.* **2011**, *50*, 7907 – 7909.
[20] Y. Bai, H. Gao, D. B. Dang, X. Y. Guo, B. An, W. L. Shang, *CrystEngComm* **2010**, *12*, 1422 – 1432.
[21] Y. Bai, C. Y. Duan, P. Cai, D. B. Dang, Q. J. Meng, *Dalton Trans.* **2005**, 2678 – 2680.
[22] Y. Bai, J. L. Wang, D. B. Dang, Y. N. Zheng, *Synth. Met.* **2012**, *162*, 2081 – 2086.
[23] Y. Bai, W. L. Shang, D. B. Dang, H. Gao, X. F. Niu, Y. F Guan, *Inorg. Chem. Commun.* **2008**, *11*, 1470 – 1473.
[24] J. H. Zhou, Y. F. Peng, Y. P. Zhang, B. L. Li, Y. Zhang, *Inorg. Chem. Commun.* **2004**, *7*, 1181 – 1183.
[25] D. B. Dang, M. M. Li, Y. Bai, R. Q. Ning, *Synth. Met.* **2012**, *162*, 2075 – 2080.
[26] Y. Bai, J. L. Wang, D. B. Dang, M. M. Li, J. Y. Niu, *CrystEngComm* **2012**, *14*, 1575 – 1581.
[27] Y. H. Fan, J. L. Wang, Y. Bai, D. B. Dang, Y. Q. Zhao, *Synth. Met.* **2012**, *162*, 1126 – 1132.
[28] D. B. Dang, W. L. Shang, Y. Bai, J. D. Sun, H. Gao, *Inorg. Chim. Acta* **2009**, *362*, 2391 – 2395.
[29] G. M. Sheldrick, *Acta Crystallogr.* **1990**, *A46*, 467 – 473.
[30] G. M. Sheldrick, *Acta Crystallogr.* **2008**, *A64*, 112 – 122.
[31] Y. Bai, X. F. Hu, D. B. Dang, F. L. Bi, J. Y. Niu, *Spectrochim. Acta, Part A, Mol. Biomol. Spectrosc.* **2011**, *78*, 70 – 73.
[32] Y. Bai, G. S. Zheng, D. B. Dang, Y. N. Zheng, P. T. Ma, *Spectrochim. Acta, Part A, Mol. Biomol. Spectrosc.* **2011**, *79*, 1338 – 1344.
[33] S. Banerjee, M. G. B. Drew, A. Ghosh, *Polyhedron* **2003**, *22*, 2933 – 2941.
[34] D. Y. Chen, H. Gao, X. F. Hu, X. Y. Guo, F. Yang, Y. Bai, *Synth. React. Inorg., Met.-Org., Nano-Met. Chem.* **2010**, *40*, 112 – 115.